Accepted Manuscript

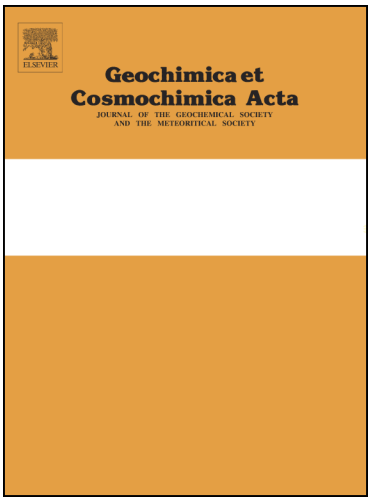

Position-Specific Hydrogen Isotope Equilibrium in Propane

Hao Xie, Camilo Ponton, Michael J Formolo, Michael Lawson, Brian K Peterson, Max K. Lloyd, Alex L Sessions, John M Eiler

PII: S0016-7037(18)30340-5
DOI: https://doi.org/10.1016/j.gca.2018.06.025
Reference: GCA 10814

To appear in: *Geochimica et Cosmochimica Acta*

Received Date: 25 January 2018
Revised Date: 18 June 2018
Accepted Date: 22 June 2018

Please cite this article as: Xie, H., Ponton, C., Formolo, M.J., Lawson, M., Peterson, B.K., Lloyd, M.K., Sessions, A.L., Eiler, J.M., Position-Specific Hydrogen Isotope Equilibrium in Propane, *Geochimica et Cosmochimica Acta* (2018), doi: https://doi.org/10.1016/j.gca.2018.06.025

This is a PDF file of an unedited manuscript that has been accepted for publication. As a service to our customers we are providing this early version of the manuscript. The manuscript will undergo copyediting, typesetting, and review of the resulting proof before it is published in its final form. Please note that during the production process errors may be discovered which could affect the content, and all legal disclaimers that apply to the journal pertain.

ACCEPTED MANUSCRIPT

Position-Specific Hydrogen Isotope Equilibrium in Propane

Hao Xie[1*], Camilo Ponton[1], Michael J Formolo[2], Michael Lawson[3], Brian K Peterson[4], Max K. Lloyd[1], Alex L Sessions[1], John M Eiler[1]

1. Division of Geological and Planetary Sciences, California Institute of Technology, Pasadena, CA, 91125, USA
2. ExxonMobil Upstream Research Company, Spring, Texas, 77389, USA
3. ExxonMobil Exploration Company, Spring, Texas, 77389, USA
4. ExxonMobil Research & Engineering, Annandale, NJ 08801, USA

* To whom the correspondence should be addressed:

Hao Xie

Division of Geological and Planetary Sciences,

California Institute of Technology,

hxie@caltech.edu

+1 626-787-4678

ACCEPTED MANUSCRIPT

Abstract

Intramolecular isotope distributions can constrain source attribution, mechanisms of formation and destruction, and temperature-time histories of molecules. In this study, we explore the D/H fractionation between central (-CH_2-) and terminal (-CH_3) positions of propane (C_3H_8) — a percent level component of natural gases. The temperature dependence of position-specific D/H fractionation of propane could potentially work as a geo-thermometer for natural gas systems, and a forensic identifier of specific thermogenic sources of atmospheric or aquatic emissions. Moreover, kinetically controlled departures from temperature dependent equilibrium might constrain mechanisms of thermogenic production, or provide indicators of biological or photochemical destruction. We developed a method to measure position-specific D/H differences of propane with high-resolution gas source mass spectrometry. We performed laboratory exchange experiments to study the exchange rates for both terminal and central positions, and used catalysts to drive the hydrogen isotope distribution of propane to thermodynamic equilibrium. Experimental results demonstrate that D/H exchange between propane and water happens easily in the presence of either Pd catalyst or Ni catalyst. Exchange rates are similar between the two positions catalyzed by Pd. However, the central position exchanges 2.2 times faster than the terminal position in the presence of Ni catalyst. At 200°C in the presence of Pd catalyst, the e-folding time of propane-water exchange is 20 days and of homogeneous exchange (i.e., equilibrium between central and terminal positions) is 28 minutes. An equilibrated (bracketed and time-invariant) intramolecular hydrogen isotope distribution was attained for propane at three temperatures, 30°C, 100°C and 200°C; these data serve as an initial experimental calibration of a new position-specific thermometer with a temperature sensitivity of 0.25‰ per ˚C at 100 ˚C. We use this calibration to test the validity of prior published theoretical predictions. Comparison of data with models suggest the most sophisticated of these discrepant

ACCEPTED MANUSCRIPT

models (Webb and Miller, 2014) is most accurate; this conclusion implies that there is a combined experimental and theoretical foundation for an 'absolute reference frame' for position-specific H isotope analysis of propane, following principles previously used for clumped isotope analysis of CO_2, CH_4 and O_2 (Eiler and Schauble, 2004; Yeung et al., 2014; Stolper et al., 2014).

1. Introduction

Non-statistical intramolecular distributions of stable isotopes have been recognized for decades. A few years after the discovery of deuterium, Koizum and Titani (1938) first studied deuterium transfer from the hydroxyl group to the benzene ring of phenol. The first study to examine natural position-specific isotopic variations in materials relevant to the Earth and life sciences measured the intramolecular carbon isotope variations of biosynthetic amino acids (Abelson and Hoering, 1961). This subject grew dramatically with the development of NMR techniques for measuring position-specific variations in D and ^{13}C abundances in organic molecules (Martin and Martin, 1981; Caytan et al., 2007). Such work has been applied to food-science, plant physiology, paleoenvironment reconstruction and environmental contamination (Remaud et al., 1997; Gilbert et al., 2012; Ehler et al., 2015; Julien et al., 2015 and 2016). Intramolecular isotopic fractionations can reflect temperatures of molecular synthesis, mechanisms of formation, and/or source substrates (Martin et al., 2008; Eiler, 2013b).

Propane (C_3H_8) is a major constituent of thermogenic natural gas. It is also the smallest alkane that has chemically non-equivalent positions, making it an attractive test case for the broader subject of intramolecular isotopic ordering. Intramolecular isotope fractionations in propane (most simply, differences in ^{13}C or D content between the central methylene and terminal methyl groups) have potential to constrain mechanisms and conditions of its formation, the chemical and biological processes of its destruction, the conditions of its migration and storage in the sub surface, and to add forensic specificity to attempts to identify sources of fugitive atmospheric and aquatic emissions. (Gilbert et al., 2016; Gao et al., 2016; Piasecki et al., 2018). An additional motivation for this study is that recent theoretical models suggest the temperature dependence of site specific hydrogen isotope fractionation in propane has promising applications to geothermometry (Webb and Miller, 2014; Cheng and Ceriotti, 2016; Piasecki et al., 2016b). Here we present an experimental study of the position-specific fractionation of D/H ratios between terminal and central hydrogen positions in propane, including methods of mass spectrometric analysis, kinetics of exchange for a range of substrates and conditions, and initial calibration of the temperature dependence of the isotope exchange reaction:

$$^{12}CH_2D-{}^{12}CH_2-{}^{12}CH_3 \rightleftharpoons {}^{12}CH_3-{}^{12}CHD-{}^{12}CH_3 \quad (1)$$

2. Background

Natural variations in the D/H ratios of hydrocarbons provide proxies for environmental conditions and water sources of biosynthesis in biomolecules (Sessions et al., 2016), source substrates and thermal maturities of catagenetically-formed oil and gas compounds (Li et al., 2001; Dawson et al., 2007), and forensic identification of environmental pollutants (Reddy et al., 2012). These stable isotope proxies are unusual both for the high amplitude of observed variations (reflecting the large relative difference in mass between H and D), and for relatively

ACCEPTED MANUSCRIPT

high susceptibility to isotopic exchange of compounds with environmental water or other compounds after formation (Schimmelman et al., 2006).

Most prior research on the hydrogen isotope compositions of natural hydrocarbons has analyzed the molecule-averaged D/H ratios of either individual compounds or bulk organic matter. Such measurements observe the weighted average of D contents of the analyzed compounds, across all non-equivalent molecular positions and for all isotopologues. Thus, they do not contain any information that might be recorded in position-specific and/or 'clumped' (multiply substituted) variations. A substantial amount of prior research establishes that such intramolecular isotopic variations can constrain the substrates, mechanisms and conditions of molecular formation, storage and destruction (e.g. Eiler, 2013b; Eiler et al., 2014). However, to-date there has been no effort to apply these principles to hydrogen isotope distributions in natural hydrocarbon gases other than methane. Here we develop a foundation to enable such studies of propane, with potential for extrapolation to other hydrocarbons.

Assuming one could observe the position-specific H isotope variations in natural propane, interpretation of such data would require at least two types of constraints: (1) the temperature dependent central-terminal fractionation at thermodynamic equilibrium, and (2) the rates of hydrogen isotope exchange between each position of propane and other materials, at naturally relevant conditions. Such data will inform the interpretation of sample measurements in the context of each sample's temperature-time history and its approach to equilibrium. Equilibrium fractionations can serve either as a calibration for thermometry in equilibrated propane, or as a reference frame for identifying and interpreting kinetic fractionations in non-equilibrated propane.

The intramolecular isotope exchange equilibrium of interest to this study (Reaction 1) can be approached by theoretical calculations or equilibration experiments. Three recent studies have presented theoretical models of this reaction (Figure A1; Webb and Miller, 2014; Cheng and Ceriotti, 2016; Piasecki et al., 2016b), using similar statistical mechanical approaches. Webb and Miller (2014) used both a Urey-Bigeleisen (i.e., rigid rotator and harmonic oscillator) model and a Path Integral Monte Carlo (PIMC) method to estimate the relevant equilibrium constant. Both methods are based on the potential energy surface (PES) used in the Chemistry at Harvard Macromolecular Mechanics (CHARMM) package. Piasecki et al. (2016b) used a Urey-Bigeleisen model, with a density function theory (DFT) model of molecular structure and vibrations. Cheng and Ceriotti (2016) used a Path Integral Molecular Dynamics (PIMD) approach, with a base molecular structure and force field that were based on the Adaptive Intermolecular Reactive Empirical Bond Order (AIREBO) force field, and which generated fundamental vibrational frequencies that differed significantly from the results of the other studies for some modes. The results of these studies are in substantial disagreement. Three of the four models (Webb and Miller, 2014 (PIMD); Webb and Miller, 2014 (Urey-Bigeleisen); Piasecki et al. (2016b) (Urey-Bigeleisen)) indicate that deuterium will be enriched in the central CH_2 groups over the terminal CH_3 groups, by an amount that diminishes monotonically with increasing temperature. In contrast, Cheng and Ceriotti, 2016 (PIMC) predict that the terminal methyl groups will be D enriched relative to the center position, with a more complex temperature dependence, increasing and then decreasing in amplitude with increasing temperature, with an inflection point near 500 K. Thus, if we can experimentally calibrate the position-specific D/H fractionation of propane as a function of temperature, we will both

ACCEPTED MANUSCRIPT

establish a new geo-thermometer and independently test the relative accuracies of these several statistical mechanical models.

The kinetics of position-specific hydrogen isotope exchange present a complex problem. Many environmental factors such as temperature, pressure, co-existing gas and fluid species and availability and properties of catalytic substrates are all likely to affect exchange rates. Studies of molecule-average D/H ratios in natural samples suggest that aliphatic compounds are resistant to hydrogen isotope exchange at near-Earth-surface conditions (Sessions et al., 2016); however, the estimated exchange half-life of 10^5~10^8 years at 100°C (Sessions et al., 2004) implies that either or both positions in propane could be 'open' to exchange for a wide range of geological times in diagenetic, catagenetic and/or metamorphic conditions. Reeves et al. (2012) reported that substantial hydrogen isotope exchange between propane and water happened on the timescale of 300 days under simulated hydrothermal conditions (323 °C and 35–36 MPa). We are not aware of any constraints on the kinetics of D/H exchange in propane at the conditions of catagenetic natural gas formation, migration, or accumulation (generally speaking, 50-200°C and 0–250 MPa).

3. Nomenclature

We report hydrogen isotope compositions using δD notation, which is defined as:

$$\delta D = \frac{\left(\frac{D}{H}\right)_{Sample}}{\left(\frac{D}{H}\right)_{Reference}} - 1 \quad (2)$$

where the D/H value is the molar ratio between deuterium (D or ^2H) and protium (H or ^1H). The δD value is generally reported in units of per mille (‰), by multiplying the quantity calculated in Eqn. 2 by 1000. The reference material is either VSMOW (D/H=0.00015576) or another material specified in the text. The position-specific fractionation factor is the difference of D/H ratios between central position and terminal positions:

$$\varepsilon_{central-terminal} = \frac{\left(\frac{D}{H}\right)_{Central}}{\left(\frac{D}{H}\right)_{Terminal}} - 1 \quad (3)$$

This quantity is also generally expressed in units of per mille after multiplication by 1000. Equation 3 assumes that D/H ratios of the central and terminal positions have been measured against the same reference composition, e.g. VSMOW. No position-specific standards are available for propane, making this approach problematic. We therefore also report a parameter for the position-specific hydrogen isotope composition of propane that can be directly related to our measurements, with minimal intervening calculations or assumptions. We report sample D/H ratios vs. our reference standard, CITP-1, which therefore has a δD_{CITP-1} of 0 for all measured or calculated properties. In practice, we analyze the relative abundance of the singly D-substituted $C_2H_5^+$ fragment ion and molecular ion ($C_3H_8^+$), obtaining the ratios, $\left(\frac{C_2H_4D}{C_2H_5}\right)$ and $\left(\frac{C_3H_7D}{C_3H_8}\right)$. At the outset of this study, we had no constraints on this standard's position-specific hydrogen isotope composition, and so we recorded the difference in D/H ratio between the central and terminal

ACCEPTED MANUSCRIPT

hydrogen sites simply as the measured difference in D/H ratio of the two measured ion species, relative to our laboratory reference gas:

$$\varepsilon D_{C2H5-C3H8} = 1000 * \left(\frac{\left(\frac{C_2H_4D}{C_2H_5}\right)_{Sample}}{\left(\frac{C_2H_4D}{C_2H_5}\right)_{CITP-1}} / \frac{\left(\frac{C_3H_7D}{C_3H_8}\right)_{Sample}}{\left(\frac{C_3H_7D}{C_3H_8}\right)_{CITP-1}} - 1 \right) \quad s(4)$$

Note that the difference in δD between the C_2H_5 and C_3H_8 species is directly related to the difference in D/H ratio between the central and terminal sites, but exhibits only 15% of the amplitude of $\varepsilon_{central-terminal}$ because the C_2H_5 and C_3H_8 ion species both contain central and terminal hydrogens, simply in different proportions (Figure 1). Specifically, the central position makes up 25% of the hydrogen atoms in the $C_3H_8^+$ molecular ion, but 40% of the hydrogen atoms in the $C_2H_5^+$ fragment ion (this fact is demonstrated experimentally in in section 4.3). Therefore, both the amplitude and measurement error in the difference in D/H ratios between the molecular and fragment ions is multiplied by approximately a factor of 6.67 when converted into the amplitude and error in position-specific D/H fractionation. When the value $\varepsilon D_{C2H5\text{-}C3H8}$ is zero, it means that the sample has a central-to-terminal D/H fractionation identical to the reference propane (CITP-1). Positive values of this index indicate that the sample is higher in $\varepsilon_{central-terminal}$ than the reference gas, and thus further to the right with respect to reaction 1(more deuteration in the central position), and vice versa.

The D/H ratios of the $C_2H_5^+$ and $C_3H_8^+$ ions can be converted into D/H ratios of the central and terminal hydrogen positions using principles of mass balance. Near the end of this paper, we use our equilibrium experiments to calibrate the true position-specific composition of our reference gas, and at that point we re-calculate absolute $\varepsilon_{central-terminal}$ and δD values of the central and terminal positions of select experimental products in the VSMOW reference frame. The conversion equations are presented in Appendix. 1.

4. Experimental

We present a new method of mass spectrometric measurements constraining the position-specific D/H ratios of propane samples. We apply that method to propane subjected to incubations across a range of temperature-pressure conditions with a variety of substrates and catalysts. This section summarizes the materials, instruments and methods used in these measurements and experiments.

4.1 Experimental Materials

4.1.1 Propane

We used two pure propane gas samples: (1) A reference propane, CITP-1, from a high-pressure cylinder of high purity propane (>99%) purchased from Air Liquide (UN1978); this is the same propane used as a reference standard by Piasecki et al., (2016a, 2018). Its bulk δD_{VSMOW} is -179±3‰, measured independently by GC-pyrolysis-MS. And (2) 98+ % pure CH_3—CD_2—CH_3 ('PROPANE (2,2-D2, 98%)') purchased from Cambridge Isotope Laboratories, Inc. This second propane was used as a deuterated 'spike' to examine the kinetics of the reaction:

$$C_3H_6D_2 + C_3H_8 \rightleftharpoons 2C_3H_7D \quad (5)$$

ACCEPTED MANUSCRIPT

We generally added 20 ppmv (by volume) of $C_3H_6D_2$ to CITP-1 for equilibrium calibration experiments on labeled gases, so that isotopic analyses of the products of these experiments would be broadly similar in molecular average D/H ratio to CITP-1. This is to minimize the effects of nonlinearity in instrumental mass fractionation (Dallas et al., 2018).

4.1.2 Water

Some experiments were conducted with deuterium-enriched water. The water was prepared by mixing 99.9 % D_2O (Cambridge Isotope Laboratories, Inc.) and deionized laboratory water by a ratio of 0.3 % volumetrically. We diluted this mixture with deionized water (reported δD_{SMOW} = -83.8 ‰) by a factor of 20.6 (by weight) in order to measure its δD on a water isotope spectroscopic analyzer (Los Gatos Research DLT-100). The measured δD_{SMOW} of the diluted mixture is 471.2±0.9 ‰, so the δD of the original mixture is 11419±31 ‰. This labeled water was used to examine the kinetics of hydrogen isotope exchange between water and propane through a reaction having a net stoichiometry (see section 4.2):

$$C_3H_8 + HDO \rightleftharpoons C_3H_7D + H_2O \quad (6)$$

4.1.3 Metal Catalysts

Some experiments were performed using either a Pd or Ni catalytic substrate. The Pd catalyst is 10 wt. % Pd on carbon from Sigma Aldrich. It is matrix-activated and carbon-supported. The reported surface area of the support is 750–1000 m^2/g. The reported average particle size is 15μm. The Ni catalyst is 65 wt. % Ni from Sigma Aldrich. The support is silica/alumina. The surface area was measured by 11-point BET analysis to be 155.93 m^2/g. Catalysts were kept in an anaerobic chamber under an N_2+3%H_2 atmosphere.

4.2 Exchange Experimental Procedures

Isotope exchange experiments were conducted by incubating propane — either CITP-1, or labeled propane (2,2 D2), or a mixture of the two, alone or in the presence of deuterated water and/or one of the catalytic substrates (Table 1). Metal catalysts are loaded in the anaerobic chamber to minimize oxidation and deactivation. Each mixture of propane ± water ± substrate was placed in a 1-2 cc Pyrex® tube. We prepared 50–70 μmol of propane, and/or 500-600 μmol of water, and 40-60 mg of substrate for the hydrous experiments and 20-30 mg of substrate for the anhydrous experiments in each sample tube. The tube was then heated to a constant temperature between 30 and 200 °C in a resistance-heated furnace, for hours to weeks. The pressure inside the tube was not controlled, but depended in a calculable way on the amounts of propane ± water in each tube, the tube volume, and the temperature of the incubation. Prior to each experiment, any catalytic substrate used in that experiment was heated by torch flame (500–600 °C) under vacuum to remove any adsorbed gas. We ceased heating when no detectable gas released from the catalyst accumulated in the gas line (<0.001 mbar in a 110 mL space for 10 seconds), which usually occurred 5-10 minutes after heating started. Then we condensed propane and water into the tube by vapor transfer through a vacuum line, with the tube immersed in liquid nitrogen. Once all reagents and catalysts were in the tube, it was flame-sealed, removed from the vacuum line and allowed to warm to room temperature. Sealed tubes were then placed in a resistance-heated oven held at a constant, monitored temperature during the incubation period. After incubation, tubes were removed from the oven and quenched in liquid nitrogen. The tubes were then opened using a tube cracker attached to a vacuum line, and propane was passed

ACCEPTED MANUSCRIPT

through a dry ice-ethanol trap to remove remaining water vapor, and then condensed in a second glass tube at -196°C (immersed in liquid N_2). This second tube was then flame-sealed and removed from the vacuum line for mass spectrometric analysis.

Table 1: A list of exchange experiments

Substrate	Propane	Water	Temperature
Ni catalyst	CITP-1	Heavy water	200°C
Pd catalyst	CITP-1	Heavy water	200°C
Pd catalyst	CITP-1	None	30°C, 100°C and 200°C
Pd catalyst	Spiked CITP-1	None	30°C, 100°C and 200°C

4.3 Mass spectrometry

All isotopic analyses of propane starting materials and experimental products were performed using a high-resolution, doubly focusing, reverse geometry, sector mass spectrometer with electron impact ionization source (a modified version of the Thermo Fischer DFS™). This instrument and its use for high-precision isotope ratio analysis are described in detail in Dallas et al. (2018). All measurements presented here used an electron impact energy of 54 eV and a filament current of 1.0 or 1.5 mA. Typically, we prepare 50–70 μmol of propane for one sample and that results in a source pressure of 6×10^{-7}~9×10^{-7} mbar.

Since this study only involves laboratory materials, our propane samples are mostly pure. Nevertheless, we confirm each sample's purity prior to isotope ratio acquisitions. First, we scan across a narrow mass range (~0.1 Dalton) at m/z=28 to monitor N_2 and CO, which are the two most common contaminants. The most abundant ion species at nominal mass 28 is $C_2H_4^+$, so we evaluate concentrations of N_2 and CO via normalizing their signal to $C_2H_4^+$. We consider the sample is contaminated by N_2 or CO if $[^{14}N_2^+]/[^{12}C_2H_4^+]$ or $[^{12}C^{16}O^+]/[^{12}C_2H_4^+]$ is higher than 1×10^{-2}. Second, we check the signal intensity of the propane molecular ion, which is $^{12}C_3H_8^+$, for the sample and CITP-1 at balanced ion source gas pressure, which can be read from the ion source gauge. Source pressure can be easily adjusted by varying inlet bellow volume. If $^{12}C_3H_8^+$ signal of the sample is within 95~100% of that of CITP-1, the discrepancy is smaller than the error of the source gauge (±5%) and we conclude that the sample is basically as clean as CITP-1. If a sample satisfies both requirements, it is ready for isotope ratio measurements. If not, we determine what the contaminant is by examining the full mass spectrum, and discard the sample.

In order to constrain the position-specific isotope difference between terminal and central hydrogen positions in propane (i.e., between CH_3— and —CH_2— groups), we require two independent observations of molecular or fragment ion species that sample different proportions of these positions (much as Yoshida (1999) and Piasecki et al. (2016a) have shown previously for position-specific measurements of ^{15}N in N_2O or ^{13}C in propane). The measurements presented here examine the D/H ratios of the full molecular ion ($C_3H_8^+$) and the ethyl fragment ion ($C_2H_5^+$). We run the DFS mass spectrometer at a tuning that delivers a mass resolution of 35,000 (FWHM), such that isobaric interferences can be well separated (Figure A2).

If $C_3H_8^+$ is produced by simple ionization and $C_2H_5^+$ is produced by simple cleavage, the full molecular ion has a ratio of terminal to central hydrogens of 3:1 and the ethyl fragment ion

ACCEPTED MANUSCRIPT

3:2. A crucial requirement of our mass-spectrometric approach is to demonstrate that $C_3H_8^+$ and $C_2H_5^+$ consistently sample these expected population of hydrogen sites from the original molecule. In order to test the validity of $C_3H_8^+$, we analyzed a sample from a second tank of propane, EM-1, using both our DFS MID method and independently using GC-pyrolysis-IRMS. The resulting δD (VSMOW) is –161.0 ± 1.0 ‰ with the DFS and –163.6 ± 3.2 ‰ with the GC-pyrolysis-IRMS. A more extensive test of these methods is in Ponton et al. (2017), which presented a cross-plot between measured δD values of natural propane samples using the DFS MID method and externally reported values (generally from GC-pyrolysis-IRMS techniques). That study confirms that the methods used here are consistent with independent constraints over a range of propane isotopic compositions in natural samples. We assume that the $C_2H_5^+$ inherits 3 of its hydrogens from the terminal methyl group of propane and 2 from the central CH_2 group. We tested our assumption regarding the $C_2H_5^+$ fragment ion by labeling the central site with two deuterium atoms (creating a strong enrichment in the otherwise rare species, $CH_3CD_2CH_3$) and then measuring the ratio, $[CD_2CH_3^+]/[^{13}C^{13}CH_5^+]$ to determine whether it is present in the expected abundance. Specifically, we added 333 ppmv of $CH_3CD_2CH_3$ into CITP-1 (known via measurements of the final D/H ratio of the mixture by GC-pyrolysis IRMS). This leads to a predicted ratio of $[CD_2CH_3^+]/[^{13}C^{13}CH_5^+]$ of 3.42. We measured this ratio at a range of source pressures spanning those commonly encountered during sample measurements (Figure A3). It is observed that $[CD_2CH_3^+]/[^{13}C^{13}CH_5^+]$ is stable to less than 3%, relative, over the source pressures of our measurements, and in all cases within 3%, relative, of the predicted value.

We apply the electric scan method and the multiple ion detection (MID) method detailed in Dallas et al., 2018. Briefly, the electric scan method involves scanning a narrow window of the accelerating voltage, observing the ion intensity at several (typically ~100) points across a mass range containing two or more ion peaks. Each scan typically takes around 1 second, and we stack multiple scans to generate a peak shape curve. The resulting peak shape curve is modeled as an additive function of the intensities of two or more peaks, in which the mass differences between these peaks are constrained. The output is interpreted through a peak-integration algorithm to obtain the ion intensity isotopologue ratios such as $[^{12}C_2H_4D^+]/[^{13}C^{12}CH_5^+]$ and $[^{12}C_3H_7D^+]/[^{13}C^{12}C_2H_8^+]$.

The MID method uses a different strategy. In this technique, ion intensities are measured by ‘jumping’ the electric accelerating voltage to the mass of the target ion, ‘parking’ on this mass for a certain time while determining its intensity, before jumping to the next selected ion. By repeating cycles of electrical jumping, we can integrate intensities of all ion peaks of interest over time. At the start of each cycle of analysis, the local mass scale is re-calibrated by two anchor peaks that envelope the target peaks. Therefore, the target mass can be jumped to precisely. In practice we use one measurement to focus on the ethyl ion isotopologues (including $[^{12}C_2H_5^+]$, $[^{13}C^{12}CH_5^+]$ and $[^{12}C_2H_4D^+]$) and another measurement to observe the molecular ion isotopologues (including $[^{12}C_3H_8^+]$, $[^{13}C^{12}C_2H_8^+]$ and $[^{12}C_3H_7D^+]$). We use $^{12}C_2H_4^+$ and O_2^+ as the anchor peaks for the ethyl ion measurement, and $^{12}C_3H_7^+$ and $^{13}C^{12}C_2H_8^+$ for the molecular ion measurement. With these measured intensities, we can calculate isotope ratios of $^{13}C/^{12}C$ and D/H independently.

Since the electric scan method measures a ratio of two near isobaric species, one containing D and the other containing 13C, it is important to investigate the possibility that the carbon isotope compositions of our experimental products changed as a result of our heating and reaction protocols. We found that exchange experiments in this study appear to have negligible

ACCEPTED MANUSCRIPT

effects on altering carbon isotope compositions of either site, at least to within limits relevant to this study. For example, a sample of CITP-1 which was exposed to Pd catalyst at 200°C on 04/07/2016, had a measured shift (end product – starting material) in $\delta^{13}C$ for the molecular ion of 0.49 ± 1.00 ‰ (2 s.e.) and for the ethyl ion of -1.00 ± 1.00 ‰ (2 s.e.). Because CITP-1 is the dominant propane component (>99.95 %) in every sample, it is a reasonable assumption that all propane samples examined in this study are uniform and equal to CITP-1 in ^{13}C content at both positions; thus, the ratios of D-bearing to ^{13}C-bearing species measured via electric scan constrain the sample/standard difference in D/H ratio for the ethyl fragment and molecular ion. In this study, most of the results are obtained via the electric scan method. The MID method is mainly used as an independent test of electric scan results.

Each measurement, using either the MID or electric scan method, comprises 10 acquisition cycles, each of which in turn spends 2.6 minutes observing the reference material (typically CITP-1, unless indicated). We obtain 10 measured sample-reference comparisons by bracketing the sample measurement with the adjacent CITP-1 measurements, and report the mean of these 10 bracketted comparisons. We report the external error of the measurement as the standard error of the ten values, as a 1 s.e. error. Each typically 1-hour measurement consumes 4–10μmol of sample gas.

5. Results

5.1 Analytical Precision and Experimental Reproducibility

Mass spectrometric precision dictates the lower limit of our analytical uncertainty. Dallas et al. (2018) showed that both the electric scan method and the MID method of isotopic analysis using the modified DFS mass spectrometer system can approach shot-noise error. Figure A4 demonstrates that the measurement error of $[^{12}C_3H_7D^+]/[^{13}C^{12}C^{12}CH_8^+]$ is only slightly greater than counting statistics. Typically, in a 1-hour D/H measurement, standard error of the ten acquisition cycles is on the order of 1‰. Converting the δD measurements of the ethyl fragment and the molecular ion into δDs of the positions leads to around 6‰ error in the central position and 3‰ error in the terminal position (See Appendix. 1 for conversion equation). Our long term analytical precision can be established by evaluating replicate measurements of the CITP-1 reference standard vs. itself (zero-enrichment tests). The measured mean δD_{C3H8} value of such tests from September 2015 to March 2017 is 0.11‰ (indistinguishable from zero), and 1 standard deviation is 1.73‰ (n=12).

Analytical reproducibility for unknown samples is established by replicating measurements of the same sample. For each sample, we repeat at least one 1-hour measurement on either the ethyl ion or the molecular ion. Sometimes a comparison between methods (electric scan method vs. MID method) is also conducted. We found that the results are replicable between measurements to within analytical error. The large majority of repeated measurement pairs have normalized error ($\frac{A-B}{\sqrt{\sigma_A^2+\sigma_B^2}}$, John and Adkins, 2010) smaller than 1.

Other possible experimental and analytical artifacts could include: (1) isotope exchange between propane and other pools of hydrogen, such as exchange with water vapor either in the incubation experiments or during ionization in the source, and exchange with absorbed hydrogen

ACCEPTED MANUSCRIPT

on metal catalytic surfaces; (2) loss of propane through thermal degradation, via decomposition reactions such as $C_3H_8 \rightarrow C_2H_4+CH_4$ (Gilbert et al., 2016); and (3) vapor loss of propane. The first source of error is controlled by passing prepared propane samples through a dry ice-ethanol cold trap. The second and the third sources of error are minimized by monitoring propane yields. We manometrically quantify the amount gas at the beginning and end of each experiment. If the pressure loss is higher than 3%, relative, we discard the sample (i.e., we only use experimental data with gas yields >97%). The purity test, as mentioned in the previous section, can also serve as a proof of sample validity.

We further characterized experimental reproducibility by repeatedly analyzing a gas prepared by adding 20 ppmv (by volume) of $CH_3CD_2CH_3$ to CITP-1. Over the course of ~1 year, we repeatedly sampled the same mixture into Pyrex® tubes and equilibrated them in the presence of Pd catalyst at either 30°C, 100°C or 200°C. After exchange, the majority (>99.9%) of deuterium exchanges to singly-deuterated propane (C_3H_7D; this is confirmed by monitoring the $C_3H_6D_2$ peak as a function of reaction time (Figure 3)). We measured these heated labeled gases against CITP-1. The main goal was to calibrate the position-specific D/H fractionation thermometer, but these data also constrain our full procedural experimental reproducibility. The difference in D/H between the equilibrated labeled gas and CITP-1, obtained by measuring $[^{12}C_3H_7D^+]$ is summarized in Table 2, which includes data of such measurements from May 2016 to April 2017.

Table 2: Experimental data set of equilibrated mixture (heated gas)

Experiment date	δD_{C3H8}	2s.e.
05/31/2016	38.1	1.5
07/31/2016	41.6	2.9
08/12/2016	37.0	3.1
08/13/2016	38.2	2.4
08/18/2016	35.2	2.6
08/20/2016	42.4	2.2
10/07/2016	37.7	2.0
11/01/2016	40.5	1.7
03/11/2017	38.9	1.8
04/03/2017	37.7	1.5

The measured replicate δD values are essentially consistent with an average of 38.74‰ (1 standard deviation = 2.19 ‰). The standard deviation does not differ significantly from the long-term instrumental precision (1.73‰, from the zero-enrichment tests), demonstrating that our catalyzed exchange experiments do not entail experimental artifacts or errors significantly in excess of mass spectrometric errors. Both heated-gas and zero-test errors are higher than the average standard error of each individual measurement (1.09‰). We suspect imperfect pressure balancing between samples and standard as a possible cause, because the software we use to control the modified DFS mass spectrometer does not support automatic pressure-adjustment.

5.2 C_3H_8-H_2O exchange

ACCEPTED MANUSCRIPT

At 200 °C, propane (CITP-1) was found to incorporate hydrogen from water over timescales of approximately 1-5 weeks in the presence of either the nickel catalyst or palladium catalyst. When exposed to deuterated water (δD=11419±31 ‰) the D/H ratio of both the central position and the terminal position increases (Figure 2). In the presence of Ni catalyst, the central hydrogens exchange significantly faster than the terminal hydrogens. In the presence of Pd catalyst there is little difference between exchange rates of the propane hydrogen positions. Hydrogen exchange in the presence of Pd catalyst is more effective than with Ni catalyst.

5.3 Internal equilibration in propane

In these experiments, two kinds of propane samples were prepared: pure CITP-1 and a mixture between CITP-1 and 20 ppmv centrally D_2-labled propane ($CH_3CD_2CH_3$). The $CH_3CD_2CH_3$ spike can provide a source of D to create a propane of different bulk hydrogen isotopic composition. In addition, it is a robust tracer for H exchange of propane, as its exchange with other propane molecules erases the excess of double-deuterated propane. By monitoring the concentration of $C_3H_6D_2$, we can assess the exchange reaction progress.

For those samples prepared from the spiked mixture, we observe decay of $C_3H_6D_2$ at all temperatures. (Figure 3) This proves that reaction 5 is progressing to the right, presumably catalyzed by Pd/C catalyst. At thermodynamic equilibrium the molar fraction of $C_3H_6D_2$ is predicted to be as low as 0.4 ppm. In these experiments we found that concentrations of $C_3H_6D_2$ reached this equilibrium value and stopped changing. Therefore, this is a strong line of evidence that the final time-invariant stages of our time-series represent the thermodynamic equilibrium state rather than the cessation of exchange due to other artifacts such as deactivation of catalyst via coke formation (e.g. Albers et al., 2001). On this basis, we conclude that it is possible to equilibrate internal hydrogen isotope ordering of propane using Pd catalyst on laboratory time scales down to room temperatures. We also learned from these experiments that equilibrating D distribution within propane molecules in the presence of Pd/C catalyst but without water happens much faster than equilibrating the propane-water-Pd/C catalyst system. Using first-order kinetics the lifetimes (e-folding times) of the excess $CH_3CD_2CH_3$ are fit to be 0.020 d at 200°C, 0.093 d at 100°C and 9.9 d at 30°C (Figure 3). Fitting this temperature dependence to the Arrhenius equation results in an activation energy of 44 kJ/mol (R^2=0.97). Sárkány et al. (1978) studied hydrogen isotope exchange between propane and D_2 gas on Pd black catalyst (precipitated elemental Pd) and found an activation energy of 58 kJ/mol, which is broadly comparable with our findings.

We observe that propane samples of different initial isotopic composition (i.e., either CITP-1 alone or the mixture of CITP-1 and $CH_3CD_2CH_3$) converge to almost identical position-specific distribution (i.e. $\varepsilon D_{C2H5\text{-}C3H8}$) at each temperature (Figure 4). On this basis, we conclude that exposure of propane to Pd catalyst reaches a time-invariant and bracketed, and thus equilibrated, state. The central-terminal fractionation appears to stabilize at a different equilibrium value for each of the three temperatures (Figure 3). To the first order, $\varepsilon D_{C2H5\text{-}C3H8}$ at equilibrium is lower at higher temperature. This indicates that D/H distribution within propane promotes greater enrichment of D in the central H site at lower temperatures.

We further tested this conclusion by creating a third, more deuterated sample by spiking the mixture with an additional 20ppmv $CH_3CD_2CH_3$ and exposing it to Pd catalyst at 200°C for 7 days. The $C_3H_6D_2$ concentration of this sample collapsed to a stochastic distribution, suggesting this mixture underwent quantitative D redistribution. Its $\varepsilon D_{C2H5\text{-}C3H8}$ is indistinguishable from the

ACCEPTED MANUSCRIPT

equilibrated original mixture and CITP-1. Table 3 lists the hydrogen isotope data for this sample and equilibrated samples of both the unspiked CITP-1 and the original 20 ppmv $C_3H_6D_2$ spiked mixture for comparison.

Table 3: Comparison of Equilibrium states of different propane samples at 200°C

Gas sample	$\delta D_{C3H8\ vs.\ CITP-1}$	1 s.e.	$\varepsilon D_{C2H5-C3H8}$	1 s.e.
CITP-1	0	N/A	12.67	1.0
CITP-1+20ppmv spike	38.0	0.8	11.24	1.2
CITP-1+40ppmv spike	74.7	1.3	11.02	2.2

6. Discussion

6.1 Position-specific exchange mechanisms

If the kinetics of hydrogen isotope exchange are treated using a pseudo first-order approximation (Robert and Urey, 1939; Sessions et al., 2004), D/H exchange rate and lifetime can be estimated through this expression:

$$e^{-kt} = \frac{F_t - F_e}{F_i - F_e} \quad (6)$$

Where F is the fraction of D among all hydrogen atoms ($D/(D+^1H)$). F_t is that fraction at time t, F_e is the fraction at equilibrium and F_i is the initial fraction. t is time, and k is the exchange rate constant, and 1/k is the e-folding time (lifetime) of this reaction. Using this equation to fit the data in Figure 2, we can obtain propane-water exchange reaction lifetimes. The molecule-averaged lifetime of exchange between propane and water is 2.8 days in the presence of Pd catalyst and 30.5 days in the presence of Ni catalyst at 200°C. Exchange rates for central position and terminal position appear to be different: In the presence of Ni catalyst, the central H exchange rate is faster than the terminal H exchange rate by a factor of 2.2. In the presence of Pd catalyst, terminal H exchanges faster by a factor of 1.3 — i.e., selectivity is detectable but reversed and less significant than for Ni catalyzed exchange. Figure 5 illustrates this difference by plotting the progress of the exchange reaction for the central site vs. that for the terminal positions. Our results for Ni catalyzed exchange are similar to what Kauder and Taylor (1951) discovered in propane-D_2 exchange. They found that the central position exchanges with D_2 gas about 3 times as fast as the terminal position exchanges in the presence of Pt catalyst.

Table 4: Fitted Propane-water hydrogen isotope exchange life times (in days) for different positions and catalysts at 200°C. R^2 indicates the goodness of fit of the first-order rate law to the data.

	Central position	R^2	Terminal position	R^2
Pd catalyst	3.4	0.899	2.6	0.975
Ni catalyst	18.4	0.982	39.1	0.996

ACCEPTED MANUSCRIPT

Three possible mechanisms have been proposed for the isotopic exchange of carbon-bound hydrogen in the light n-alkanes. The first is a radical exchange mechanism, in which the position-specific exchange rates are dependent on the bond dissociation energies (BDE) for each position. The BDE difference between central position and terminal position of propane is -10.7 kJ/mol (Luo, 2007). Under this scenario, we can estimate the ratio of position-specific exchange rates using the Arrehnius equation,

$$\frac{k_{central}}{k_{terminal}} = \frac{A_{central}}{A_{terminal}} e^{\frac{E_{terminal}-E_{central}}{RT}} \quad (7)$$

where E stands for the activation energy for each hydrogen position, and A the frequency factors for the positions. It has been shown that frequency factor ratios are generally close to one (e.g. Ranzi et al., 1997), so we assume that the frequency factors are the same between the central position and the terminal position. Taking the BDE difference into account and assuming a temperature of 200 °C, we obtain that $k_{central}/k_{terminal}$ = 15.2. The central hydrogen exchange is strongly favored in this case since the secondary alkyl radical (i.e. –CH·–) is much more stable than the primary radical (i.e. $–CH_2·$). A second possibility is di-adsorption, which includes αα, αβ and αγ types(Sattler, 2018). Bond (2006) suggests that αβ is the favored exchange mechanism for small straight-chain alkanes. Under this mechanism, each swap of hydrogen atoms involves one central hydrogen position and one terminal hydrogen position. Since the symmetry number ratio between central position and terminal position is 2/6, $k_{central}/k_{terminal}$=3. Thus, this mechanism also predicts faster central exchange and slower terminal exchange. A third possibility is ionic exchange, which is involves the dissociation of either proton or hydride (Schimmelmann et al., 2006; Sattler, 2018). Alexander et al. (1984) reported that alkyl H exchange happens exclusively on the position adjacent to the position that is more stable for carbocation. Since the secondary carbocation is much more stable than primary, the mechanism favors the exchange on the terminal position. Robertson et al. (1975) studied ionic exchange between propane and D_2 on the surface of γ-alumina and found that the central position of propane exchanges 170 times faster than the terminal position. Hence, ionic exchange is the only plausible mechanism that would prefer terminal exchange over central exchange.

We plotted the predicted trajectories for these mechanisms in a plot of the δD of CH_2 groups vs. δD for methyl groups in Figure 5. We conclude from the data presented in Figure 5 that metal-catalyzed exchange is a mixture of multiple mechanisms. The Ni catalyzed exchange experiments has $k_{central}/k_{terminal}$=2.2, closely approaching the predictions of the αβ di-adsorption mechanism ($k_{central}/k_{terminal}$=3), suggesting it dominates on that catalyst, but is perhaps accompanied by a minor contribution of ionic exchange. This is consistent with Bond's (2006) review. The Pd catalyzed experiments suggest a greater role for ionic exchange and reduced importance of radical or αβ di-adsorption mechanisms. However, other combinations of these three mechanisms are permitted by our data.

6.2 Position-specific hydrogen isotope fractionation at thermodynamic equilibrium

We conclude that our exchange experiments examining internal hydrogen isotope exchange of propane constrain the equilibrium central-terminal fractionation to be the final, common value to which both the CITP-1 and spiked CITP-1 experimental series converge. This

ACCEPTED MANUSCRIPT

allows us to obtain the equilibrium $\varepsilon D_{C2H5\text{-}C3H8}$ values. In order to determine when the propane samples are equilibrated for each temperature, we use the exchange rates learned from observing decay of $CH_3CD_2CH_3$ (Figure 3). We use the filter of >5 e-folding times to select the equilibrated samples, which is equivalent to >99.3% completion of exchange reaction. As a result, we have 6 data points for 30°C, 7 for 100°C and 8 for 200°C. We average these 'equilibrated' experiments at each temperature.

Figure 6 presents our experimental data along with all four previously published theoretical predictions for the center-terminal hydrogen isotope fractionation in propane, using units that allow us to directly compare all five sets of constraints (four models and our data) on a common plot. A comparison of these data is informative despite the fact that our measurements describe only relative differences between experimental products and an intralaboratory standard. In the left panel of figure, we re-normalize all four theoretical predictions and our experiment to each of their fractionation at a temperature of 200˚C, and then examine the changes in predicted and observed values for the fractionation at lower temperatures. Three of the four predictions are within 2s.e. errors of our experimental data: both models presented by Webb and Miller (2014) and the model presented by Piasecki et al. (2016b). Cheng and Ceriotti's result falls outside the 2s.e. error limits of our data at both 30˚C and 100˚C.

There are several possible explanations for the difference between the Cheng and Ceriotti model and the other three we consider, but there is reason to believe it reflects an error in the potential energy surface (PES) in the model of Cheng and Ceriotti. The models of Webb and Miller (2014) and Cheng and Ceriotti (2014) used path-integral methods, but employed different PESs for integration. Cheng and Ceriotti (2014) used the Adaptive Intermolecular Reactive Empirical Bond Order (AIREBO) force field whereas Webb and Miller (2014) used the Chemistry at Harvard Macromolecular Mechanics (CHARMM) PES. These two models derive dramatically different vibrational frequencies for the fundamental modes of propane. In Table A1 we list the vibrational frequencies of propane isotopomers derived from the two PESs (AIREBO and CHARMM), as well as those predicted by a density function theory with a B3LYP-6311G** basis set, shown for comparison. The CHARRMM frequencies are generally consistent with those predicted by B3LYP-6311G**. In the modes 5-19, there is a large difference between frequencies calculated by the AIREBO model and the other two model estimates. AIREBO frequencies can be as much as 500 cm^{-1} higher than CHARRMM frequencies. Such a conflict is beyond the magnitude of common errors. Additionally, we compared AIREBO frequencies of $^{12}C_3H_8$ with spectroscopically measured fundamental modes for propane (Table A1) and the same discrepancy exists. The AIREBO frequencies are much higher than observation in the middle frequency range. We suggest that the AIREBO PES used by Cheng and Ceriotti is likely responsible for the discrepant behavior of Cheng and Ceriotti's PIMC calculations.

Three observations suggest that our experimental data serve as a calibration of the propane D/H position-specific thermometer: Our findings are time-independent after an initial exchange period; our findings are bracketed (independent of initial composition); and the temperature-dependence of the fractionation we observe is consistent with the consensus of several theoretical predictions (recognizing the one discrepant prediction). We conclude that at thermodynamic equilibrium, D prefers to be in the central position of propane, and the central-terminal enrichment decreases with increasing temperature. The model that most closely matches

ACCEPTED MANUSCRIPT

our experimental findings is the PIMC model presented by Webb and Miller (2014). If we use our experimental products as a reference frame (following the reasoning behind the clumped isotope absolute reference frames for CO_2, CH_4, N_2O and O_2 (Eiler and Schauble, 2004; Yeung et al., 2014; Stolper et al., 2014)), we can calculate the hydrogen isotope structure of CITP-1: $\delta D_{central\_SMOW} = -208.3 \pm 6.6‰$ and $\delta D_{terminal\_SMOW} = -169.2 \pm 3.5‰$ and $\varepsilon_{central-terminal} = -47.1 \pm 8.9‰$.

6.3 A kinetic model of metal catalyzed exchange processes

Our experimental findings indicate hydrogen isotope exchange involving propane molecules over laboratory time scales at temperatures of 30-200 ˚C in the presence of Pd/C catalyst. However, it is difficult to use these results as precise constraints on the rate constants of this exchange both because some combinations of time and temperature have little data coverage (e.g., 30 ˚C at short times), and because multiple reaction mechanisms may be involved in re-distributing D within and between propane molecules. Nevertheless, it is worth asking whether our results are consistent with a defined set of exchange reactions having rates and activation energies broadly consistent with the results of our kinetic experiments (above). For this reason, we present a hypothesized model for the mechanisms and rates of H isotope exchange in propane, and examine whether that model is internally consistent and matches our experimental findings.

We constructed a three-box model to simulate the exchange kinetics and equilibria. The three boxes represent three hydrogen pools: the central position of propane, the terminal position of propane and absorbed hydrogen on a catalytic metal surface (Figure 7).

In this model, we describe hydrogen isotopic exchange on a Pd surface as governed by the following isotopic exchange reactions:

$$CH_3CD_2CH_3 + \text{Pd-H} \rightleftarrows CH_3CHDCH_3 + \text{Pd-D} \qquad \text{(k1, 8)}$$

$$CH_3CHDCH_3 + \text{Pd-H} \rightleftarrows CH_3CH_2CH_3 + \text{Pd-D} \qquad \text{(k2, 9)}$$

$$CH_3CH_2CH_2D + \text{Pd-H} \rightleftarrows CH_3CH_2CH_3 + \text{Pd-D} \qquad \text{(k3, 10)}$$

Please note that each of these reactions represent net reactions of several elementary steps. For example, the forward reaction of k1 is combined from of two elementary steps: $CH_3CD_2CH_3 + Pd \rightarrow CH_3CDPdCH_3 + \text{Pd-D}$ and $CH_3CDPdCH_3 + \text{Pd-H} \rightarrow CH_3CHDCH_3 + Pd$. We define k_n and K_n to be the forward rate constants and equilibrium constants for the n^{th} reaction. The following differential equations can be derived:

$$\frac{d[CH_3CD_2CH_3]}{dt} = k_1[CH_3CD_2CH_3][Pd-H] - k_1/K_1 * [CH_3CHDCH_3][Pd-D] \qquad (11)$$

$$\frac{d[CH_3CHDCH_3]}{dt} = -k_1[CH_3CD_2CH_3][Pd-H] + k_1/K_1 * [CH_3CHDCH_3][Pd-D] - k_2[CH_3CHDCH_3][Pd-H] + k_2/K_2 * [CH_3CH_2CH_3][Pd-D] \qquad (12)$$

$$\frac{d[CH_3CH_2CH_2D]}{dt} = -k_3[CH_3CH_2CH_2D][Pd-H] + k_3/K_3 * [CH_3CH_2CH_3][Pd-D] \qquad (13)$$

ACCEPTED MANUSCRIPT

$$\frac{d[Pd-D]}{dt} = k_1[CH_3CD_2CH_3][Pd-H] - \frac{k_1}{K_1} * [CH_3CHDCH_3][Pd-D] + k_2[CH_3CHDCH_3][Pd-H] - \frac{k_2}{K_2} * [CH_3CH_2CH_3][Pd-D] + k_3[CH_3CH_2CH_2D][Pd-H] - \frac{k_3}{K_3} * [CH_3CH_2CH_3][Pd-D] \quad (14)$$

We numerically solved this family of equations with MATLAB®. The unknown variables in this model include k_1, k_2, k_3, K_1, K_2, K_3 and relative sizes of the absorbed hydrogen reservoir. The constraints that permit us to solve for these variables are as follows:

First, exchange rate constants of the central position and the terminal position have been reported in Section 6.1. We assume the reaction rate ratio between the central position and the terminal position does not depend on whether or not water is present and is independent of temperature. Therefore, we can apply the same relationship, $k_2/k_3 = 0.76$ (Table 4), here. Second, k_2/k_1 is an H/D secondary kinetic isotope effect, because it describes the effect of isotopic substitution on one of the central positions on the dissociation rate of the other. For covalent C-H bonds, the secondary kinetic isotope effect is close to unity, commonly in the range of 0.8~1.2 (e.g., Lu et al., 1990), so we set k_2/k_1 equal to 1 in the model. Finally, for this purpose the effect of isotope clumping (i.e., the propensity of heavy isotopes to bond together) is trivial. We approximate that equilibrium concentrations of isotopologues follow the stochastic rule. This approximation adds a constraint on the equilibrium constants: $K_2/K_1=4$.

With these controls, there are four free variables left: k_1, K_1, K_3 and the relative size of the surface hydrogen reservoir. We fit the model to the experimental data set (i.e., time variations in abundances of the various measured species). Results are shown in Figure 8. The model outputs are consistent with the data within experimental precision. This model predicts that CH_3CHDCH_3 will rise faster than $CH_3CH_2CH_2D$ when $CH_3CD_2CH_3$ is being consumed. It is because the first step of $CH_3CD_2CH_3$ exchange with the catalyst-bound H pool generates a CH_3CHDCH_3 molecule. This leads to faster changes in the $\varepsilon D_{C2H5\text{-}C3H8}$ value of spiked gas relative to un-spiked gas, with even a slight overshoot in the early period of spiked gas exchange. The faster rise of $\varepsilon D_{C2H5\text{-}C3H8}$ value of spiked gas is well observed in experimental data. (Figure 8).

We re-iterate that the details of our model are under constrained with respect to time and temperature sampling points and should be considered only an approximate statement about the rate constants for D/H exchange within and between propane molecules. However, this exercise shows that our experimental findings are internally consistent with a simple and intuitive description of the family of reaction steps involved in this process.

6.4 Implications for the interpretation of data for natural propanes

This study examines hydrogen isotope exchange of propane in the presence of artificial metal catalysts that are not common in nature. Therefore, it is reasonable to consider whether propane is too refractory to H isotope exchange to equilibrate its isotopic structure in natural settings. Interpretation of the bulk molecular D/H ratio of propane (and other natural gas

ACCEPTED MANUSCRIPT

hydrocarbons) assumes this property is immune to hydrogen isotope exchange between hydrocarbon molecules and molecular positions (e.g. Tang et al., 2005; Ni et al., 2011). However, our findings indicate that intramolecular exchange of H between terminal and central positions in propane under anhydrous conditions occurs orders of magnitude faster than exchange between propane and water. Thus we might expect that propane in natural crustal environments could internally re-equilibrate its position-specific hydrogen isotope structure even in the absence of changes in molecule averaged δD. We should also consider that even if propane fails to reach H isotope exchange equilibrium with co-existing hydrous compounds in geological conditions, our findings indicate that partial exchange may lead to a signature in hydrogen isotope site preference that constrains the thermal stress (time-at-temperature) and/or exposure to catalysts propane experienced since its formation. We show that intermolecular hydrogen isotope exchange rates (i.e., between propane and water) can differ between central and terminal hydrogen positions, depending on the co-existing catalysts. In particular, the central position exchanges hydrogen isotopes approximately twice as fast as the terminal position when Ni catalyst is present. The difference in exchange rates of the positions can lead to significant variance in central-to-terminal fractionation as propane approaches equilibrium with water (or perhaps another hydrous compound; Figure 5). Interpretation of natural propane samples' position-specific D/H will have to take this phenomenon into account. Future studies should examine the exchange kinetics for propane in the presence of natural catalysts (e.g. minerals or rocks) to establish whether these conclusions based on metal catalyzed experiments are truly generalizable.

More generally, we anticipate that several processes will complicate the interpretation of position-specific hydrogen isotope fractionation in propane as a thermometer to natural systems. Radical chain reactions involving other hydrocarbons (Xiao, 2001) and microbial gas degradation (Jaekel et al., 2014) are two common processes that likely involve irreversible, isotopically fractionating elementary kinetic steps. In fact, we should expect that some small amount of propane destruction by irreversible 'cracking' occurred during our experiments, but had no apparent isotopic effects because the accompanying equilibration reactions happened on much faster timescales than propane destruction (this is demonstrably obvious; our experiments lose a negligible fraction of propane over a time scale equivalent to many e-folding times of exchange – see Figure 3). It also should be noted that even in natural systems dominated by irreversible elementary kinetic reactions, an interconnected network of such reactions can drive systems to or near equilibrium molecular and isotope distributions if they indirectly interconvert different compounds (and their isotopic forms). Such systems are said to have reached 'metathetic equilibrium', and are hypothesized to be common in natural gas forming systems (Mango et al., 2010). This study provides a foundation to test these hypotheses with measurements of position-specific hydrogen isotope fractionations in propane from natural gases and pyrolysis experiments. Our reference propane, CITP-1, which comes from a commercial gas supplier, is significantly D-depleted in the central position relative to its terminal position ($\varepsilon_{\text{central}-\text{terminal}}$ = -47.1±8.9‰). Its position-specific D/H distribution is far from internal equilibrium. This finding is comparable to NMR results from Liu et al. (2018), where they measured $\delta D_{central}$- $\delta D_{terminal}$ = –26.4±8.8‰ in a commercially obtained propane. These data suggest that some common process can easily generate large position-specific disequilibria. This phenomenon strengthens the prospect of applying this tool to study the origin and evolution of natural propane, as it suggests that both non-equilibrium and equilibrium signatures are possible (and thus might distinguish between different formation mechanisms and environments).

ACCEPTED MANUSCRIPT

7. Conclusions

We have developed a method to analyze position-specific D/H variations of propane via high-resolution mass spectrometry. The same methodology, which involves measuring D/H ratios of specific fragment ions, should be amenable to the measurement of other small hydrocarbon molecules.

In a series of incubation experiments, we measured catalyzed hydrogen exchange kinetics of propane. Our results document differences in effectiveness between Ni and Pd catalysts and differences in the relative rates of exchange for the two non-equivalent hydrogen positions. The exchange rates we observe do not exactly match any one previously proposed mechanism, suggesting our experiments involved exchange by two or more mechanisms. We also observed that the exchange between propane and water is slower than propane internal exchange in an anhydrous environment. We experimentally produced propane with an equilibrated position-specific hydrogen isotopic structure. The position-specific hydrogen isotope equilibrium in propane was shown to be time-invariant, composition-bracketed and mass-balanced to within a few percent at three temperatures. Our results are able to discriminate between several different theoretical predictions, ruling out the one that predicts terminal position D enrichment. We conclude that our data serve as a calibration of the position-specific propane D/H thermometer. In the range of natural gas formation and storage, the fractionation factor is highly sensitive to temperature (around 0.25‰ per ˚C at 100 °C). With commercially available multi-collector high resolution mass spectrometers (e.g. Eiler et al., 2013a), we anticipate that we will be able to improve the precision of position-specific measurements by approximately an order of magnitude relative to the work presented here, and therefore should be able to apply this thermometer with a precision of 2~5°C in the range of geological relevant temperatures.

Acknowledgements

This research is supported by an NSF-EAR instruments and facilities grant and Caltech. Additional funding is provided by Exxon Mobil. We thank Michael Webb and Thomas Miller for helpful discussions and for providing the vibrational frequency calculations for the empirical PES. We thank Aaron Sattler and Michele Paccagnini for insightful advices on catalytic chemistry. We thank Nami Kitchen for advice and assistance with the experimental setup and the operation of the DFS mass spectrometer.

ACCEPTED MANUSCRIPT

References

ACCEPTED MANUSCRIPT

Abelson P. H. and Hoering T. C. (1961) Carbon isotope fractionation in formation of amino acids by photosynthetic organisms. *Proceedings of the National Academy of Sciences.* 47(5): 623-32.

Albers P., Pietsch J. and Parker S. F. (2001) Poisoning and deactivation of palladium catalysts. *J. Mol. Catal. A Chem.* **173**, 275–286.

Alexander R., Kagi R. I. and Larcher A. V (1984) Clay catalysis of alkyl hydrogen exchange reactions—reaction mechanisms. *Org. Geochem.* **6**, 755–760.

Bond G. C. (2005) *Metal-catalysed reactions of hydrocarbons*., Springer.

Caytan E., Remaud G. S., Tenailleau E. and Akoka S. (2007) Precise and accurate quantitative 13 C NMR with reduced experimental time. *Talanta* **71**, 1016–1021.

Cheng B. and Ceriotti M. (2014) Direct path integral estimators for isotope fractionation ratios. *J. Chem. Phys.* **141**, 244112.

Dallas B., Eiler J. M., Clog M., Ponton C., Xie H., Griep-Raming J., Schweiters J. and Kitchen N. (submitted) High precision stable isotope analysis of molecular and fragment ions using a high resolution, single-collector mass spectrometer. (2017)

Dawson D., Grice K., Alexander R. and Edwards D. (2007) The effect of source and maturity on the stable isotopic compositions of individual hydrocarbons in sediments and crude oils from the Vulcan Sub-basin, Timor Sea, Northern Australia. *Org. Geochem.* **38**, 1015–1038.

Ehlers I., Augusti A., Betson T. R., Nilsson M. B., Marshall J. D. and Schleucher J. (2015) Detecting long-term metabolic shifts using isotopomers: CO2-driven suppression of photorespiration in C3 plants over the 20th century.

Eiler J. M. (2013) The isotopic anatomies of molecules and minerals. *Annu. Rev. Earth Planet. Sci.* **41**, 411–441.

Eiler J. M., Bergquist B., Bourg I., Cartigny P., Farquhar J., Gagnon A., Guo W., Halevy I., Hofmann A. and Larson T. E. (2014) Frontiers of stable isotope geoscience. *Chem. Geol.* **372**, 119–143.

Eiler J. M., Clog M., Magyar P., Piasecki A., Sessions A., Stolper D., Deerberg M., Schlueter H.-J. and Schwieters J. (2013) A high-resolution gas-source isotope ratio mass spectrometer. *Int. J. Mass Spectrom.* **335**, 45–56.

Eiler J. M. and Schauble E. (2004) 18 O 13 C 16 O in Earth's atmosphere. *Geochim. Cosmochim. Acta* **68**, 4767–4777.

ACCEPTED MANUSCRIPT

ACCEPTED MANUSCRIPT

Gao L., He P., Jin Y., Zhang Y., Wang X., Zhang S. and Tang Y. (2016) Determination of position-specific carbon isotope ratios in propane from hydrocarbon gas mixtures. *Chem. Geol.* **435**, 1–9.

Gilbert A., Yamada K., Suda K., Ueno Y. and Yoshida N. (2016) Measurement of position-specific 13 C isotopic composition of propane at the nanomole level. *Geochim. Cosmochim. Acta* **177**, 205–216.

Jaekel U., Vogt C., Fischer A., Richnow H.-H. and Musat F. (2014) Carbon and hydrogen stable isotope fractionation associated with the anaerobic degradation of propane and butane by marine sulfate-reducing bacteria. *Environ. Microbiol.* **16**, 130–140.

John S. G. and Adkins J. F. (2010) Analysis of dissolved iron isotopes in seawater. *Mar. Chem.* **119**, 65–76.

Julien M., Nun P., Robins R. J., Remaud G. S., Parinet J. and Höhener P. (2015) Insights into Mechanistic Models for Evaporation of Organic Liquids in the Environment Obtained by Position-Specific Carbon Isotope Analysis. *Environ. Sci. Technol.* **49**, 12782–12788.

Julien M., Nun P., Höhener P., Parinet J., Robins R. J. and Remaud G. S. (2016) Enhanced forensic discrimination of pollutants by position-specific isotope analysis using isotope ratio monitoring by 13 C nuclear magnetic resonance spectrometry. *Talanta* **147**, 383–389.

Kauder L. N. and Taylor T. I. (1951) Experiments on the Catalytic Exchange of Acetone and Propane with Deuterium. Science **113(2931)**, 238-241.

Koizumi M. and Titani T. (1938) Austauschreaktion der Kernwasserstoffatome des Phenols. I. Austauschreaktion in alkalischer Lösung. *Bull. Chem. Soc. Jpn.* **13**, 681–690.

Li M., Huang Y., Obermajer M., Jiang C., Snowdon L. R. and Fowler M. G. (2001) Hydrogen isotopic compositions of individual alkanes as a new approach to petroleum correlation: case studies from the Western Canada Sedimentary Basin. *Org. Geochem.* **32**, 1387–1399.

Liu C., Mcgovern G. P. and Horita J. (2015) Position-Specific Hydrogen and Carbon Isotope Fractionations of Light Hydrocarbons by Quantitative NMR. In *AGU Fall Meeting Abstracts*

Lorant F., Prinzhofer A., Behar F. and Huc A.-Y. (1998) Carbon isotopic and molecular constraints on the formation and the expulsion of thermogenic hydrocarbon gases. *Chem. Geol.* **147**, 249–264.

Lu D. H., Maurice D. and Truhlar D. G. (1990) What is the effect of variational optimization of the transition state on. alpha.-deuterium secondary kinetic isotope effects? A prototype: CD3H+ H. dblarw. CD3+ H2. *J. Am. Chem. Soc.* **112**, 6206–6214.

Luo Y.-R. (2007) *Comprehensive handbook of chemical bond energies*., CRC press.

ACCEPTED MANUSCRIPT

Mango F. D. and Jarvie D. M. (2010) Metathesis in the generation of low-temperature gas in marine shales. *Geochem. Trans.* **11**, 1.

Martin G. J. and Martin M. L. (1981) Deuterium labelling at the natural abundance level as studied by high field quantitative 2H NMR. *Tetrahedron Lett.* **22**, 3525–3528.

Martin G. J., Martin M. L. and Remaud G. (2008) SNIF-NMR—Part 3: From Mechanistic Affiliation to Origin Inference. In *Modern Magnetic Resonance* Springer. pp. 1669–1680.

Ni Y., Ma Q., Ellis G. S., Dai J., Katz B., Zhang S. and Tang Y. (2011) Fundamental studies on kinetic isotope effect (KIE) of hydrogen isotope fractionation in natural gas systems. *Geochim. Cosmochim. Acta* **75**, 2696–2707.

Park R. and Epstein S. (1961) Metabolic fractionation of C13 & C12 in plants. *Plant Physiol.* **36**, 133.

Piasecki A., Sessions A., Lawson M., Ferreira A. A., Neto E. V. S. and Eiler J. M. (2016a) Analysis of the site-specific carbon isotope composition of propane by gas source isotope ratio mass spectrometer. *Geochim. Cosmochim. Acta* **188**, 58–72.

Piasecki A., Sessions A., Lawson M., Ferreira A. A., Neto E. V. S., Ellis G. S., Lewan M. D. and Eiler J. M. (2018) Position-specific 13C distributions within propane from experiments and natural gas samples. *Geochim. Cosmochim. Acta* **220**, 110–124.

Piasecki A., Sessions A., Peterson B. and Eiler J. (2016b) Prediction of equilibrium distributions of isotopologues for methane, ethane and propane using density functional theory. *Geochim. Cosmochim. Acta* **190**, 1–12.

Ponton C., Xie H., Lawson M., Formolo M., Peterson B., Sattler A. & Eiler J. (2017) *Goldschmidt Abstracts*, **2017** 3194

Ranzi E., Faravelli T., Gaffuri P., Garavaglia E. and Goldaniga A. (1997) Primary pyrolysis and oxidation reactions of linear and branched alkanes. *Ind. Eng. Chem. Res.* **36**, 3336–3344.

Reddy C. M., Arey J. S., Seewald J. S., Sylva S. P., Lemkau K. L., Nelson R. K., Carmichael C. A., McIntyre C. P., Fenwick J. and Ventura G. T. (2012) Composition and fate of gas and oil released to the water column during the Deepwater Horizon oil spill. *Proc. Natl. Acad. Sci.* **109**, 20229–20234.

Reeves E. P., Seewald J. S. and Sylva S. P. (2012) Hydrogen isotope exchange between n-alkanes and water under hydrothermal conditions. *Geochim. Cosmochim. Acta* **77**, 582–599.

Remaud, G.S., Martin, Y.L., Martin, G.G. and Martin, G.J., 1997. Detection of sophisticated adulterations of natural vanilla flavors and extracts: application of the SNIF-NMR method to vanillin and p-hydroxybenzaldehyde. *Journal of Agricultural and food Chemistry* **45**(3), pp.859-866.

ACCEPTED MANUSCRIPT

Richet P., Bottinga Y. and Javoy M. (1977) A Review of Hydrogen, Carbon, Nitrogen, Oxygen, Sulphur, and Chlorine Stable Isotope Fractionation Among Gaseous Molecules. *Annu. Rev. Earth Planet. Sci.* **5**, 65–110.

Roberts I. and Urey H. C. (1939) Kinetics of the exchange of oxygen between benzoic acid and water. *J. Am. Chem. Soc.* **61**, 2580–2584.

Robertson P. J., Scurrell M. S. and Kemball C. (1975) Exchange of alkanes with deuterium over [gamma]-alumina. A Bronsted linear free energy relationship. *J. Chem. Soc. Faraday Trans. 1 Phys. Chem. Condens. Phases* **71**, 903–912.

Sattler A. (2018) Hydrogen/Deuterium (H/D) Exchange Catalysis in Alkanes. *ACS Catal.* **8**, 2296–2312.

Sárkány A., Guczi L. and Tétényi P. (1978) Reactions of some alkanes on palladium black catalyst. *ACTA Chim. Acad. Sci. HUNGARICAE* **96**, 27–37.

Schimmelmann A., Sessions A. L. and Mastalerz M. (2006) Hydrogen isotopic (D/H) composition of organic matter during diagenesis and thermal maturation. *Annu. Rev. Earth Planet. Sci.* **34**, 501–533.

Sessions A. L., Sylva S. P., Summons R. E. and Hayes J. M. (2004) Isotopic exchange of carbon-bound hydrogen over geologic timescales. *Geochim. Cosmochim. Acta* **68**, 1545–1559.

Sessions A. L. (2016) Factors controlling the deuterium contents of sedimentary hydrocarbons. *Org. Geochem.* **96**, 43–64.

Shimanouchi, T. (1972) *Tables of Molecular Vibrational Frequencies Consolidated Volume I*; National Bureau of Standards: Washington, DC 126.

Stolper D. A., Sessions A. L., Ferreira A. A., Neto E. V. S., Schimmelmann A., Shusta S. S., Valentine D. L. and Eiler J. M. (2014) Combined 13 C–D and D–D clumping in methane: Methods and preliminary results. *Geochim. Cosmochim. Acta* **126**, 169–191.

Tang Y., Huang Y., Ellis G. S., Wang Y., Kralert P. G., Gillaizeau B., Ma Q. and Hwang R. (2005) A kinetic model for thermally induced hydrogen and carbon isotope fractionation of individual n-alkanes in crude oil. *Geochim. Cosmochim. Acta* **69**, 4505–4520.

Webb M. A. and Miller III T. F. (2014) Position-specific and clumped stable isotope studies: Comparison of the Urey and path-integral approaches for carbon dioxide, nitrous oxide, methane, and propane. *J. Phys. Chem. A* **118**, 467–474.

Xiao Y. (2001) Modeling the Kinetics and Mechanisms of Petroleum and Natural Gas Generation: A First Principles Approach. *Rev. Mineral. Geochemistry* **42**, 383–436.

ACCEPTED MANUSCRIPT

ACCEPTED MANUSCRIPT

Yeung L. Y., Ash J. L. and Young E. D. (2014) Rapid photochemical equilibration of isotope bond ordering in O_2. *J. Geophys. Res. Atmos.* **119**, 10552–10566.

ACCEPTED MANUSCRIPT

ACCEPTED MANUSCRIPT

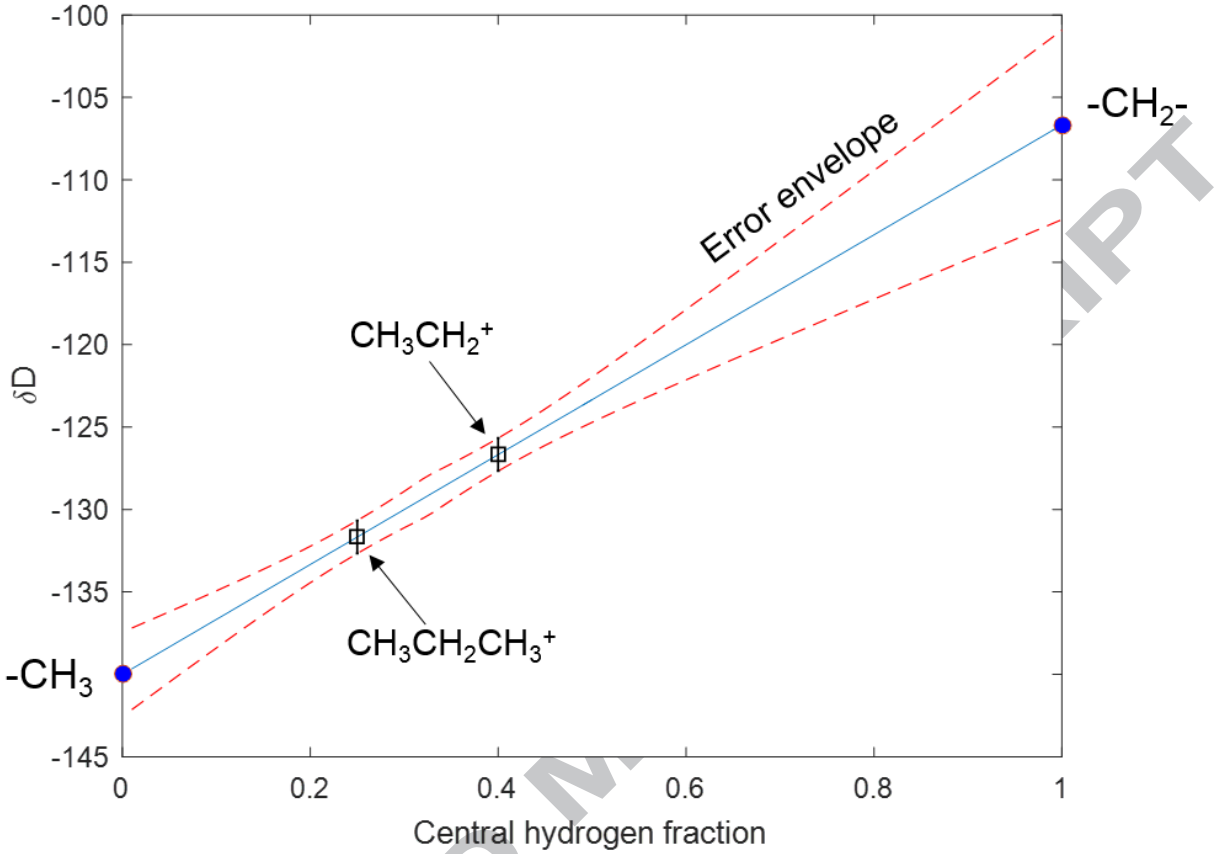

Figure 1: An illustration of the relationship between site-specific hydrogen isotope fractionation in propane and the isotopic contrast between molecular and ethyl fragment ions. The x-axis shows the fraction of hydrogen in a measured species that comes from the central site. The molecular ion contains 2/8=0.25 central hydrogen and the ethyl fragment contains 2/5=0.4 central hydrogen. A line connecting these two values can be extrapolated to obtain the endmember hydrogen isotope compositions of the central and terminal sites. This extrapolation leads to a magnification of analytical errors, as shown.

ACCEPTED MANUSCRIPT

ACCEPTED MANUSCRIPT

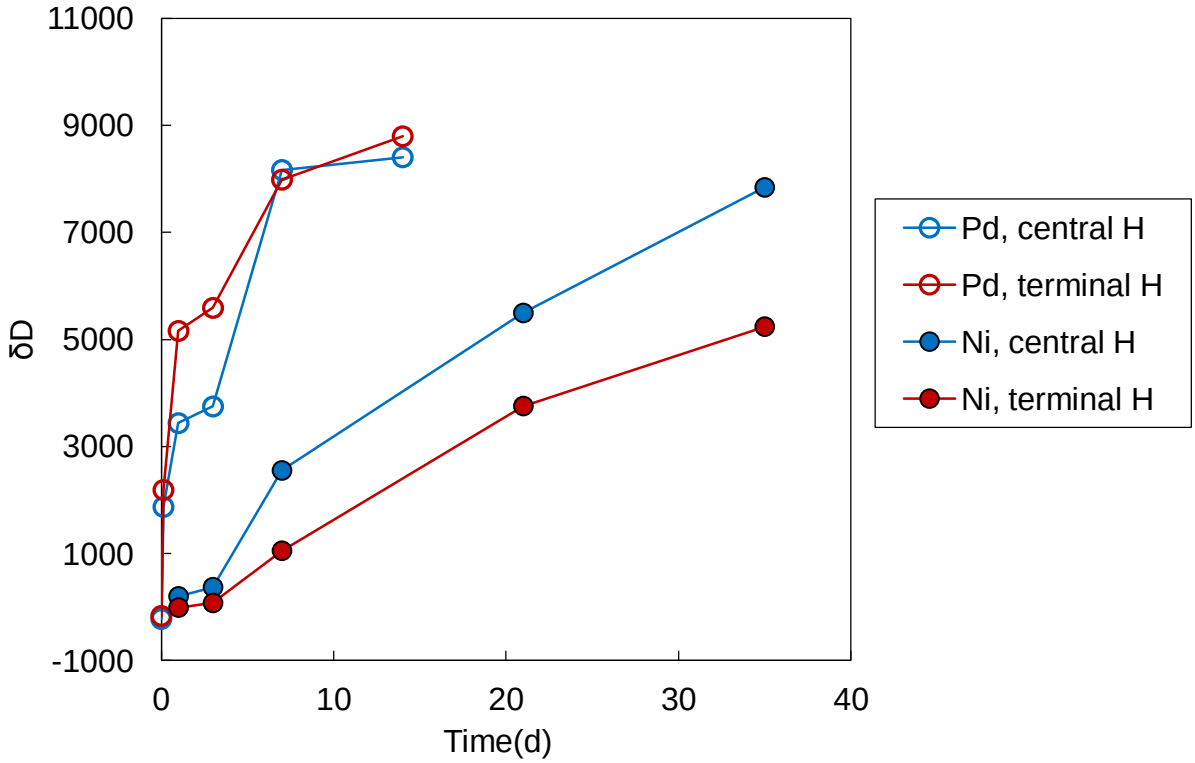

Figure 2 : δD values (vs. VSMOW) for central and terminal hydrogens of propane after reacting with deuterated water at 200°C, in the presence of Ni catalyst or Pd catalyst. We cannot confidently establish systematic errors associated with measurements of very D-rich samples, but estimate it could be as high as 100‰ for central H and 50‰ for terminal H. The scale conversion from CITP-1 to VSMOW is done with the known position-specific D/H ratios of CITP-1; see Appendix. A for details.

ACCEPTED MANUSCRIPT

ACCEPTED MANUSCRIPT

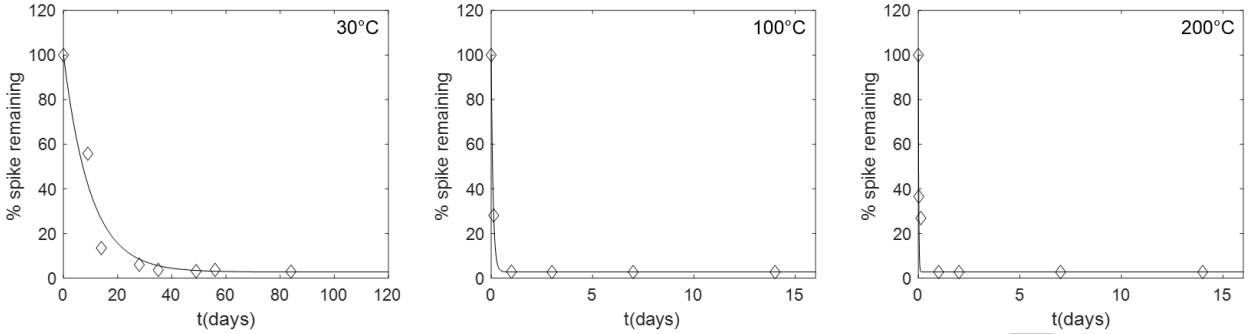

Figure 3: The change in concentrations of the spike $CH_3CD_2CH_3$ during anhydrous exchange experiments at three different temperatures. The spike concentrations are normalized to their original value prior to the experiments, i.e. $100\% \times [CH_3CD_2CH_3]_t/[CH_3CD_2CH_3]_0$. The diamonds are experimental data and the lines represent least square fits using first order kinetics.

ACCEPTED MANUSCRIPT

ACCEPTED MANUSCRIPT

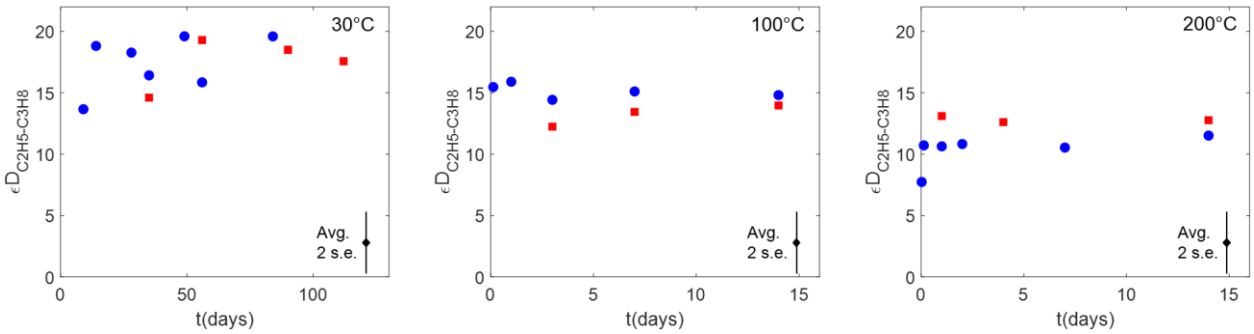

Figure 4: Time-series for measures of propane site-specific hydrogen isotope fractionation over the course of experiments in which propane is exposed to Pd catalyst at each of three controlled temperatures. Two initial propane compositions are used: CITP-1 (solid squares) and CITP-1 spiked with 20ppmv $CH_3CD_2CH_3$ (solid circles). The vertical axis represents the difference in dD between the ethyl fragment and molecular ions, which is proportional to the difference in dD between the central and terminal hydrogen sites. The average analytical uncertainty, reported as 2 standard errors (±2.8‰), is shown in the bottom right corner of each panel. Raw data and errors are available in the electronic appendix accompanying this paper.

ACCEPTED MANUSCRIPT

ACCEPTED MANUSCRIPT

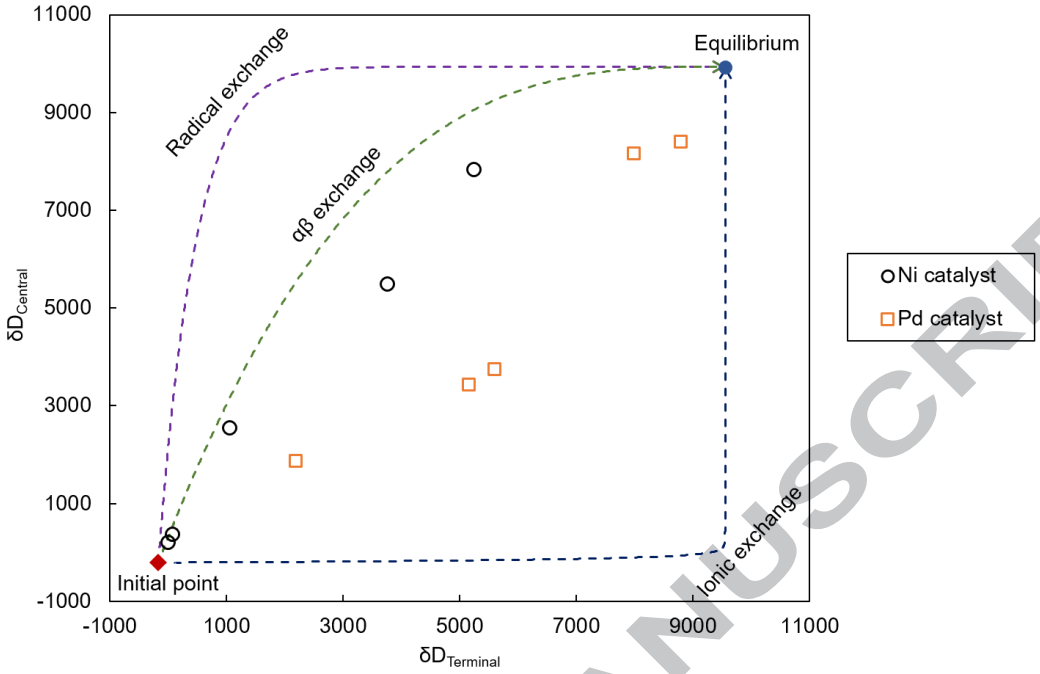

Figure 5: Evolution in the δD of terminal and central hydrogen sites of propane, observed in our experiments, and predicted trajectories for three proposed mechanisms of hydrogen isotope exchange: (1) radical exchange (2) αβ di-adsorption; (3) ionic exchange. The hydrogen isotope composition of propane in equilibrium with water vapor is calculated using results of Piasecki et al., 2016b and Richet et al., 1977.

ACCEPTED MANUSCRIPT

ACCEPTED MANUSCRIPT

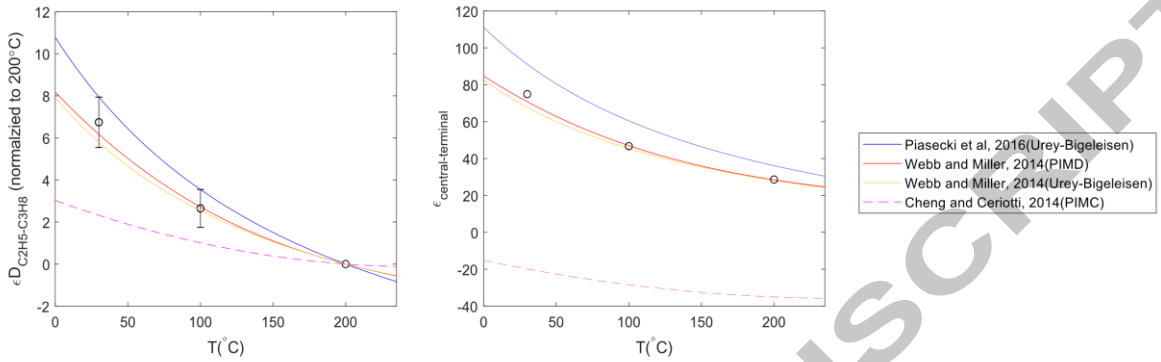

Figure 6: The measured equilibrium site-specific hydrogne isotope fractionation in propane plotted vs. temperature and compared to various theoretical predictions. The left panel shows the difference between the ethyl and molecular ions, which is normalized to such difference at 200°C in order to remove the dependence on the assumed intramolecular D/H fractionation in the CITP-1 standard. The right panel expresses these same data as the equilvant difference in D/H between the central and terminal positions, assuming the central position of CITP-1 has a $\delta D = -208.3‰$ and the terminal position of CITP-1 has $\delta DSMOW = -169.2‰$. (see text for details). Error bars reflect 2 standard errors of the mean of the equilbrated samples at each temperature. (n=6 for 30°C data, n=7 for 100°C data and n=8 for 200°C data). The path-integral methods (PIMC and PIMD) only report fractionation factors for 3-6 temperature points, so we fitted their data to second order polynomial functions to interpolate fractionation factors at all temperature in this range.

ACCEPTED MANUSCRIPT

ACCEPTED MANUSCRIPT

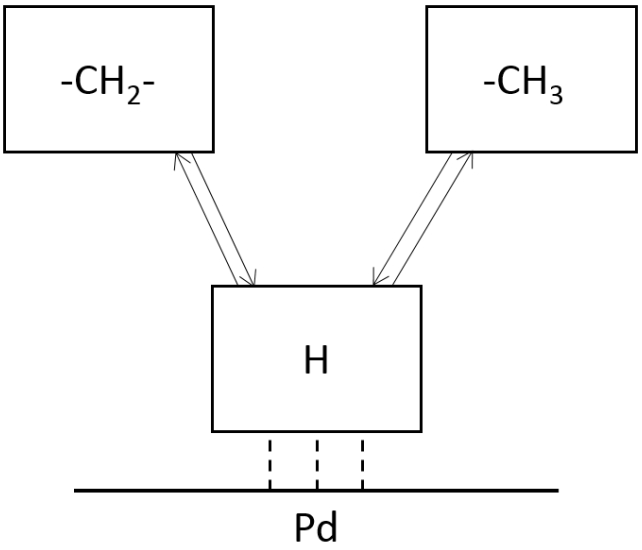

Figure 7: Idealized hydrogen isotope exchange scheme of the three-box model used to fit our data for internal isotope exchange in propane. The main hydrogen reservoirs in this model are: central hydrogen, terminal hydrogen and absorbed hydrogen.

ACCEPTED MANUSCRIPT

ACCEPTED MANUSCRIPT

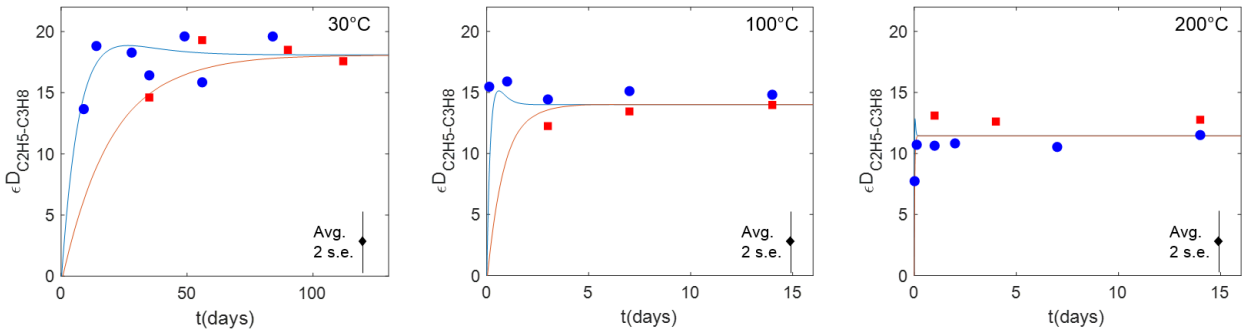

Figure 8: Fits of our three-box model to experimental results. The solid circles and solid squares represent the position-specific hydrogen isotope fractionation of spiked CITP-1 and pure CITP-1, respectively. The solid blue lines and solid red lines represent the optimized model for position-specific hydrogen isotope fractionation of spiked CITP-1 and pure CITP-1, respectively (converted into the units used for the Y axis; i.e., expressed as the difference between ethyl and molecular ions, normalized to CITP-1).

ACCEPTED MANUSCRIPT

ACCEPTED MANUSCRIPT

ACCEPTED MANUSCRIPT

ACCEPTED MANUSCRIPT

Appendix Figures

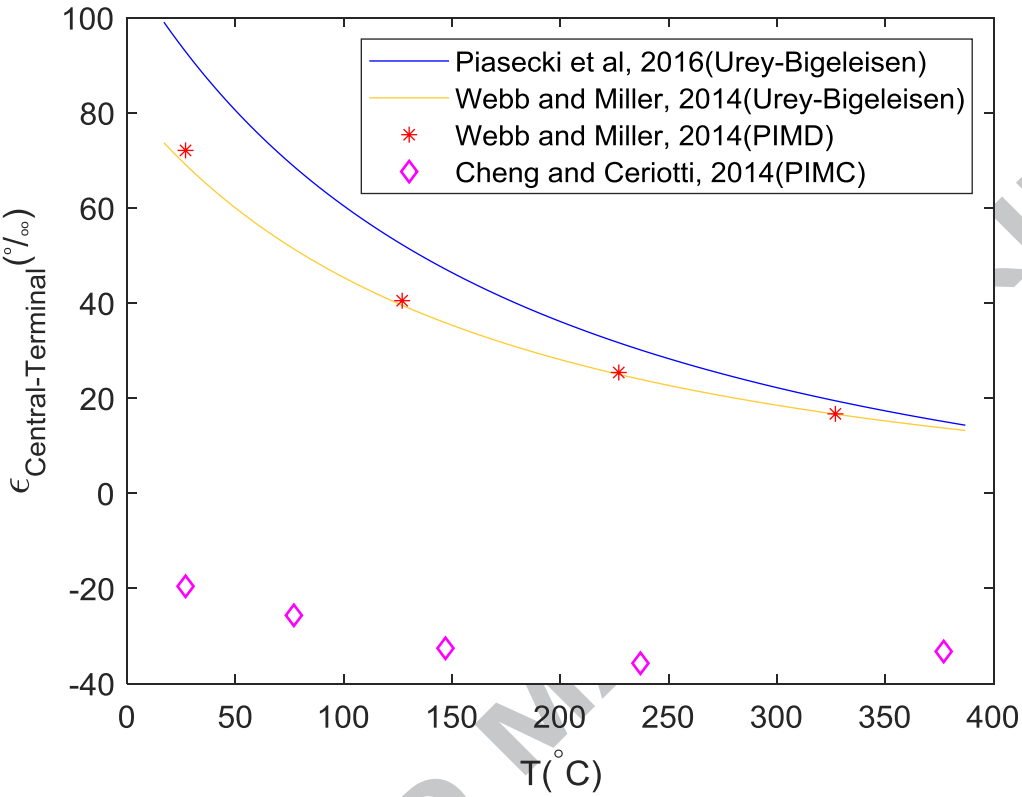

Figure A1: Comparison of model predictions of the temperature dependence of the central-to-terminal hydrogen isotope fractionation factor for propane. PIMD stands for "Path Integral Molecular Dynamics" and PIMC stands for "Path Integral Monte Carlo".

ACCEPTED MANUSCRIPT

ACCEPTED MANUSCRIPT

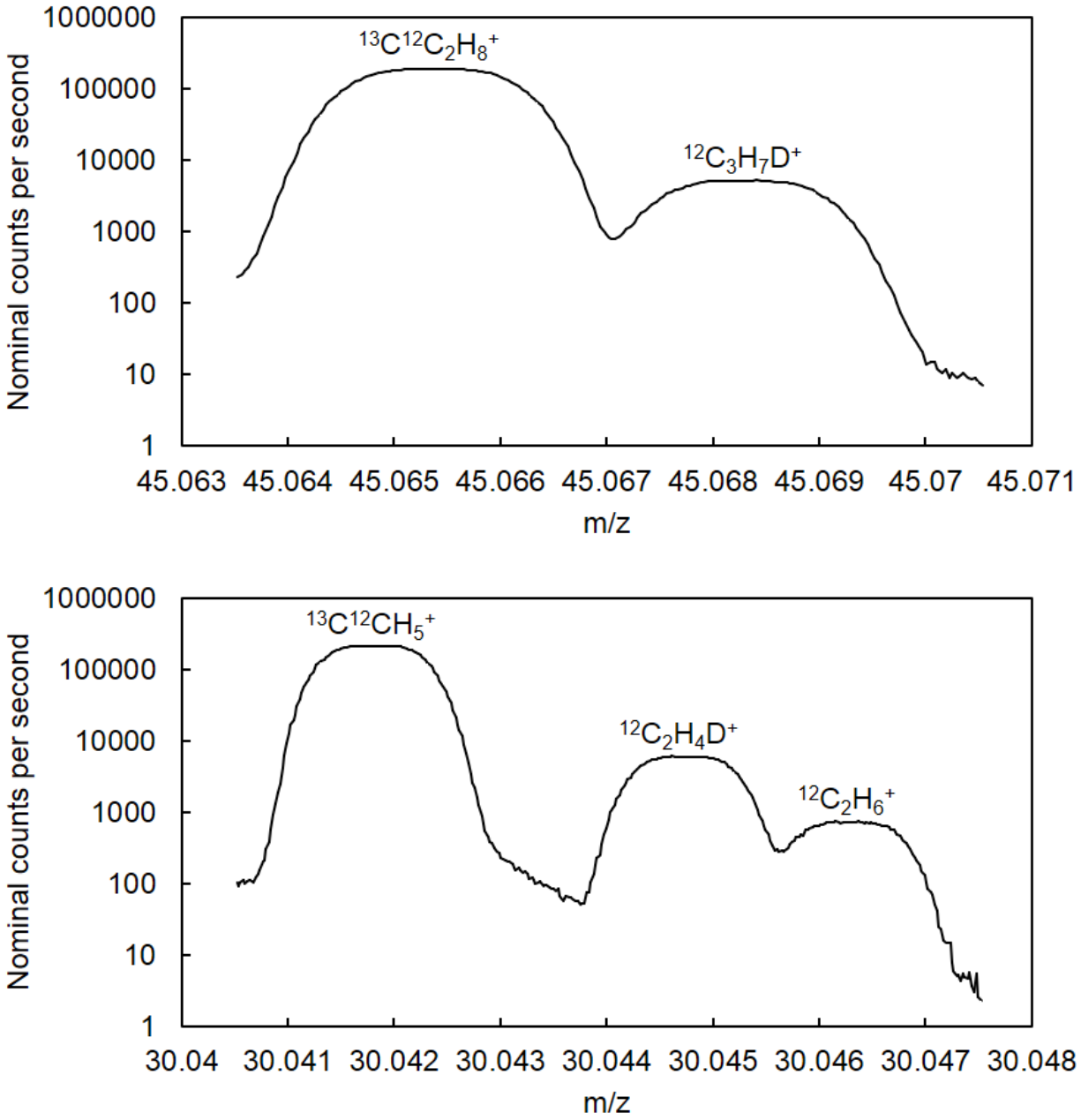

Figure A2 Local mass spectrum of m/z=45 species (up) and m/z=45 species (bottom).

ACCEPTED MANUSCRIPT

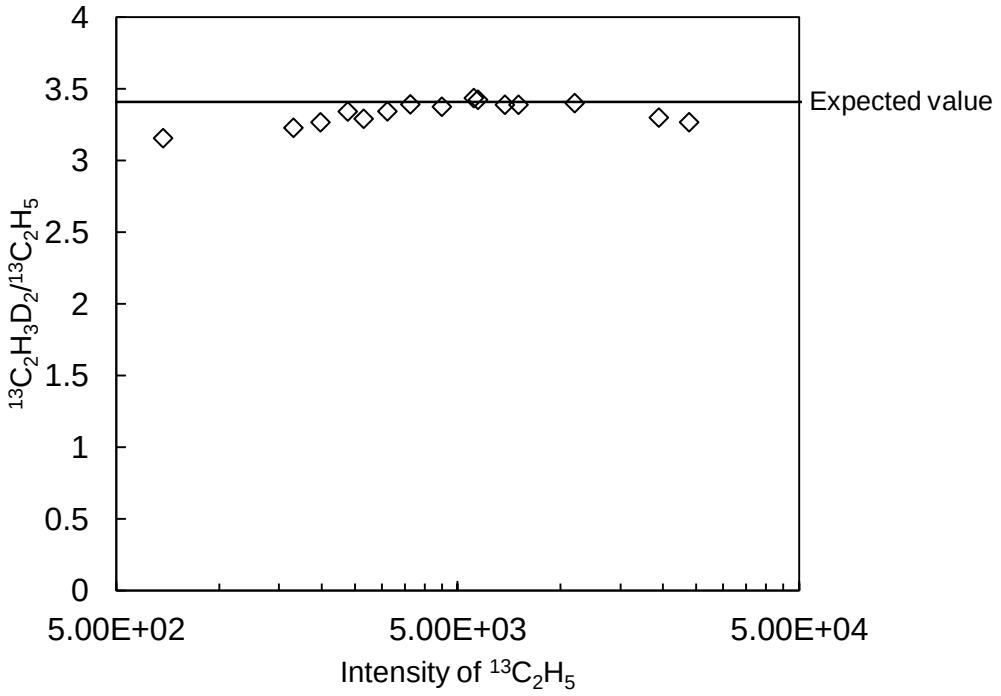

Figure A3: Tests of our hypothesis regarding the sources of hydrogen (central vs. terminal sites) in the ethyl fragment ion. The X-axis is the intensity in units of counts/s. and the Y-axis is the relative concentration of $^{13}C_2H_3D_2$. We varied the pressure in the ion source to generate a range in ion intensity. Open squares are measurements and the horizontal solid line is calculated based on the known mixing ratio of $CH_3CD_2CH_3$ in the analyzed gas.

ACCEPTED MANUSCRIPT

ACCEPTED MANUSCRIPT

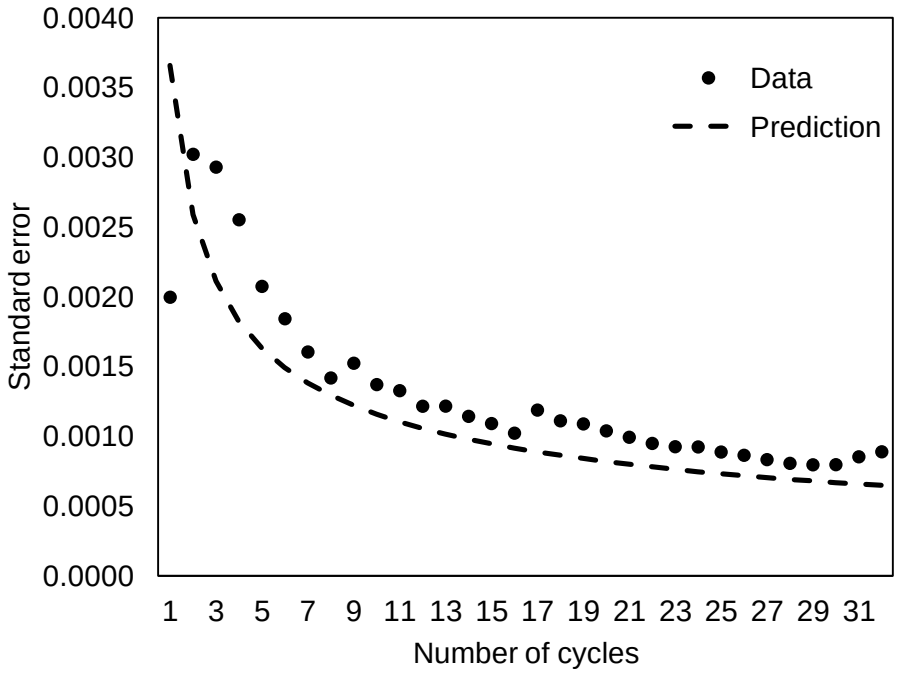

Figure A4: The results of a test of whether the measurement error is limited by counting statistics. The plots show the external error of the measured $[^{12}C_3H_7D^+]/[^{13}C^{12}C^{12}CH_8^+]$ ratio, made via the electric scan method; the dashed curve indicates the predicted evolution of errors across multiple analytical cycles for the case where errors are shot noise limited. Each cycle is 2.3 minutes.

ACCEPTED MANUSCRIPT